



ELSEVIER

Journal of Alloys and Compounds xxx (2006) xxx–xxx

Journal of
ALLOYS
AND COMPOUNDS

www.elsevier.com/locate/jallcom

Infrared spectrum and compressibility of Ti_3GeC_2 to 51 GPa

Bouchaib Manoun^{a,*}, H. Yang^a, S.K. Saxena^a, A. Ganguly^b, M.W. Barsoum^b,
Z.X. Liu^c, M. Lachkar^d, B. El Bali^e

^a Center for Study of Matter at Extreme Conditions (CeSMEC), Florida International University, VH-140, University Park, Miami, FL 33199, USA

^b Department of Materials Science and Engineering, Drexel University, Philadelphia, PA 19104, USA

^c U2A Beamline, Bldg. 725B, National Synchrotron Light Source, Brookhaven National Laboratory, Upton, NY 11973-5000, USA

^d Laboratoire d'Analyses, d'Essais et d'Environnement (LAEE), Dept de Chimie, Fac. des Sciences 'Dhar Mehraz',

Universite' Sidi Mohamed Ben Abdellah, 30000 Fes, Morocco

^e Laboratory of Mineral Solid and Analytical Chemistry "LMSAC", Department of Chemistry, Faculty of Sciences, University Mohamed I, Oujda, Morocco

Received 11 May 2006; received in revised form 12 June 2006; accepted 13 June 2006

Abstract

Using a synchrotron radiation source and a diamond anvil cell, we measured the pressure dependence of the lattice parameters of a polycrystalline Ti_3GeC_2 sample up to a pressure of 51 GPa. No phase transformations were observed. As for Ti_3SiC_2 , and most other compounds belonging to the same family of ternary carbides and nitrides, the so-called MAX phases, the compressibility of Ti_3GeC_2 along the c axis is greater than that along the a axis. The bulk modulus is 197 ± 4 GPa, with a pressure derivative of 3.4 ± 0.1 . We also characterized Ti_3GeC_2 by infrared spectroscopy; four of the five expected infrared modes were observed for this material.

© 2006 Published by Elsevier B.V.

Keywords: High pressure; MAX phases; Ti_3GeC_2 ; Infrared spectroscopy

1. Introduction

Since the discovery that the ternary compounds with the $\text{M}_{n+1}\text{AX}_n$ (MAX) chemistry, where $n = 1, 2$ or 3 , M is an early transition metal, A is an A-group (mostly IIIA and IVA) element and X is C or N possess an unusual, and sometimes unique, set of properties, they have been studied extensively [1–10]. In these phases, near close-packed transition metal carbide and/or nitride layers are interleaved with layers of pure A-group elements. In general these phases are good thermal and electrical conductors, and are relatively soft (Vickers hardness ≈ 2 – 5 GPa). They are also quite damage, thermal shock and fatigue resistant. Probably the most important and unusual characteristic of the MAX phases, however, is their machinability; they are most readily machinable with regular high-speed tool steel with no coolant or lubricant required. Such an unusual combination of properties derives partially from the metallic nature of the bonding, partially from their layered structure, and partly from

the fact that basal plane dislocations are mobile at all temperatures.

Of special interest to this work is Ti_3GeC_2 , which was first synthesized in the late 1960s in powder form [11]. This carbide adopts a hexagonal crystal structure, which consists of layers of edge sharing TiC_6 octahedra and a square-planar Ge layer [11]. The edge sharing TiC_6 octahedra are identical to those found in the rock-salt structure of the corresponding binary carbide, TiC . It was not until recently, however, that single phase fully dense bulk samples were fabricated and characterized [12,13]. Like its isostructural cousin, Ti_3SiC_2 , which has been extensively studied, Ti_3GeC_2 is relatively soft, a good thermal and electrical conductor and machinable.

In a recent diamond anvil cell study [14], the bulk modulus of Ti_3GeC_2 was investigated under a non-hydrostatic state of stress up to 64 GPa. Evidence for a shear-induced phase transformation at ≈ 26.6 GPa was reported. The bulk modulus was calculated to be 179 ± 10 GPa. Further, the compressibilities along the a and c axes did not display much of an anisotropy, and differed from the anisotropies observed in Ti_3SiC_2 [15] and $\text{Ti}_3\text{Si}_{0.5}\text{Ge}_{0.5}\text{C}_2$ [16].

One of the motivations of this work was to measure the compressibility of Ti_3GeC_2 under nearly hydrostatic conditions and

* Corresponding author. Tel.: +1 305 348 3445; fax: +1 305 348 3070.
E-mail address: manounb@fiu.edu (B. Manoun).



Table 1
Unit cell parameters and volume of Ti_3GeC_2 at various pressures

P (GPa)	a (Å) ± 0.002	c (Å) ± 0.02	V (Å ³) ± 0.1	V/V_0	ala_0	clc_0
0	3.084	17.80	146.6	1	1	1
2.54	3.074	17.70	144.8	0.987	0.9966	0.9942
6.10	3.054	17.55	141.8	0.967	0.9904	0.9862
12.06	3.027	17.47	138.7	0.946	0.9816	0.9816
16.64	3.007	17.32	135.7	0.925	0.9751	0.9733
22.37	2.989	17.17	132.8	0.906	0.9691	0.9649
24.17	2.980	17.20	132.3	0.902	0.9661	0.9665
28.95	2.967	17.08	130.2	0.888	0.9619	0.9599
34.99	2.953	16.86	127.3	0.868	0.9576	0.9471
39.32	2.940	16.80	125.8	0.858	0.9532	0.9441
43.24	2.929	16.75	124.4	0.849	0.9496	0.941
47.10	2.918	16.58	122.2	0.834	0.9460	0.9317
51.16	2.904	16.59	121.2	0.827	0.9417	0.9320

compare our results to the recent studies [14]. We also report on the infrared spectrum of Ti_3GeC_2 , which, as far as we are aware, is a first for any MAX phase.

2. Experimental procedure

The sample processing details can be found elsewhere [13]. In brief, bulk polycrystalline samples of Ti_3GeC_2 were prepared by hot pressing the appropriate stoichiometric composition of Ti, graphite and Ge powders at 1873 K for 6 h with an applied pressure of 45 MPa. The samples were then annealed at 1873 K for 48 h in an Ar atmosphere.

Powdered samples were pressurized using a gasketed diamond anvil cell (DAC) with a 400 μm culet. The gasket made of Rhenium, with 250 μm in initial thickness, indented to about 50 μm , and had a 150 μm diameter hole. Al was used as the pressure-transmitting medium and as marker. The details can be found elsewhere [16–22]. The pressure was determined from the equation of state of Al [23].

The room temperature X-ray diffraction measurements were carried out using an angle dispersive synchrotron radiation at CHESS (Cornell University), with a wavelength of $\lambda = 0.496$ Å. Diffraction rings were recorded between $2\theta = 1^\circ$ and 35° . FIT2D software [24,25] was employed to convert the image plate records into 2θ 's and intensities. The cell parameters were determined using least squares refinement on individually fitted peaks. The peaks were assigned to the hexagonal structure with the space group $P6_3/mmc$; a few impurity peaks of low intensity were also observed and ignored.

The IR measurements were performed at U2A beamline of the National Synchrotron Light Source, Brookhaven National Laboratory. The optical layout of the beamline facility has been described in detail elsewhere [26,27]. The spectra were collected with a Bruker IFS 66v/S vacuum Fourier transform interferometer, Bruker IRscope II microscope equipped with HgCdTe type-A detector for mid-IR and custom made vacuum IR microscope with Bolometer detector for far-IR. The synchrotron source was used for both far- and mid-IR measurements. The optical bench was evacuated and the microscope was purged with dry N_2 gas during the measurements to reduce or eliminate absorption by water vapor. The resolution for all the measurements is 4 cm^{-1} with 1024 scans for mid-IR and 512 scans for far-IR, respectively. The second set of experiment (far-IR) was taken from a thin film with thickness $< 1\ \mu\text{m}$, which was generated by squeezing a small amount of sample powder with a diamond anvil cell. This enhanced the signal to noise ratio of the absorption measurements.

3. Results and discussion

The lattice parameters, unit cell volumes, V , and their relative changes with pressure are listed in Table 1. Least-squares fit of the changes in the relative unit cell volume, V/V_0 , with pressure

(Fig. 1) yields:

$$\frac{V}{V_0} = 1 - 0.0046 \frac{P}{P_0} + 3 \times 10^{-5} \left(\frac{P}{P_0} \right)^2 \quad R > 0.998 \quad (1)$$

where $P_0 = 1$ GPa, V_0 is the unit cell volume (146.6 ± 0.1 Å³) at $P = 1$ atm.

Fitting the same results to the Birch-Murnaghan equation [28]:

$$P = \frac{3}{2} K_0 \left[\left(\frac{V}{V_0} \right)^{-7/3} - \left(\frac{V}{V_0} \right)^{-5/3} \right] \times \left\{ 1 + \frac{3}{4} (K'_0 - 4) \left[\left(\frac{V}{V_0} \right)^{-2/3} - 1 \right] \right\} \quad (2)$$

yields a K_0 value of 197 ± 2 GPa, with a derivative, K'_0 of 3.4 ± 0.1 . While this K_0 value is 17% greater than the value determined from ultrasound experiments on bulk Ti_3GeC_2 [29],

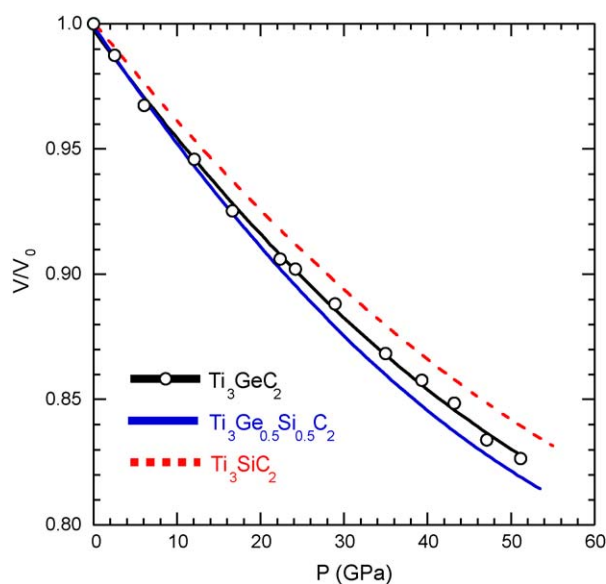


Fig. 1. Effect of pressure on relative unit cell volume, V/V_0 , of Ti_3GeC_2 . Also shown are the results for Ti_3SiC_2 and $\text{Ti}_3\text{Si}_{0.5}\text{Ge}_{0.5}\text{C}_2$ taken from Refs. [15] and [16], respectively.

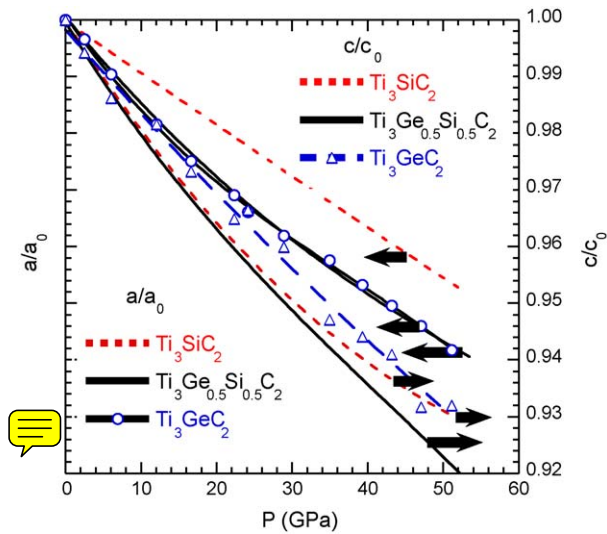


Fig. 2. Pressure dependencies of the a/a_0 (left axis) and c/c_0 (right axis) for Ti_3GeC_2 (symbols), Ti_3SiC_2 (dashed lines) and $\text{Ti}_3\text{Si}_{0.5}\text{Ge}_{0.5}\text{C}_2$ (solid lines) [15,16].

it is in excellent accord with recent *ab initio* calculations, which predict K_0 to be 198 GPa [30]. This value is greater than that (179 ± 10 GPa) reported for a nominally identical sample measured in a diamond anvil cell under non-hydrostatic conditions [14], but less than that for Ti_3SiC_2 [15] (206 GPa) or TiC (220 GPa) [31].

The P - V curves of Ti_3SiC_2 and $\text{Ti}_3\text{Si}_{0.5}\text{Ge}_{0.5}\text{C}_2$ are also plotted in Fig. 1 for comparison. Clearly Ti_3GeC_2 is more compressible than Ti_3SiC_2 but less than $\text{Ti}_3\text{Si}_{0.5}\text{Ge}_{0.5}\text{C}_2$. It follows that the substitution of Ge for Si in Ti_3SiC_2 leads to a modest softening. Interestingly, the solid solution is more compressible than the two end members. This conclusion is consistent with the thermal expansion results, which show that the solid solution exhibits a larger thermal expansion than its end members [29].

The pressure dependencies of the lattice parameters are plotted in Fig. 2; least squares fits of the curves yield:

$$\frac{a}{a_0} = 1 - 0.0016 \left(\frac{P}{P_0} \right) + 9 \times 10^{-6} \left(\frac{P}{P_0} \right)^2 \quad R > 0.998 \quad (3)$$

and

$$\frac{c}{c_0} = 1 - 0.0016 \left(\frac{P}{P_0} \right) + 5 \times 10^{-6} \left(\frac{P}{P_0} \right)^2 \quad R > 0.992 \quad (4)$$

Not surprisingly, like Ti_3SiC_2 and $\text{Ti}_3\text{Si}_{0.5}\text{Ge}_{0.5}\text{C}_2$, Ti_3GeC_2 is more compressible along the c than along the a -axis.

Based on first-principles total energy calculations, Wang and Zhou [32] suggested that a reversible polymorphic phase transition is possible in Ti_3SiC_2 at high shear strains. They described it as a sliding of Si atoms between the 2b and 2d Wyckoff positions. Wang et al. [14] recently showed that indeed when Ti_3GeC_2 was subjected to a non-hydrostatic state of stress, a phase transformation was observed at ≈ 27 GPa. The results of this work are

consistent with this view: in the absence of shear stresses, no phase transformation was observed.

Based on group theory analysis we predict the following modes for the M_3AX_2 structure: $2A_{1g} + 4A_{2u} + 3E_{2g} + 4E_{1u} + 2E_{1g}$. Of these, $2A_{1g} + 3E_{2g} + 2E_{1g}$ are Raman active; $3A_{2u} + 2E_{1u}$ are infrared active, and $A_{2u} + 2E_{1u}$ are acoustic modes. The synchrotron infrared spectrum of Ti_3GeC_2 is shown in Fig. 3. Four of the five predicted modes are observed. The peaks observed at 210.4, 252.3 and 340.5 cm^{-1} (Fig. 3a) are close to those calculated for Ti_3SiC_2 viz. 175, 270 and 318 cm^{-1} , respectively. The far-IR peak observed, as strong reflection, (Fig. 3b) around 875 cm^{-1} is higher than that predicted for Ti_3SiC_2 at 607 cm^{-1} , it may be attributed to multiphonon absorptions. These comments notwithstanding it is hereby acknowledged that the assignment of these modes is preliminary and has to be complemented and verified by more experiments and theoretical calculations for Ti_3GeC_2 .

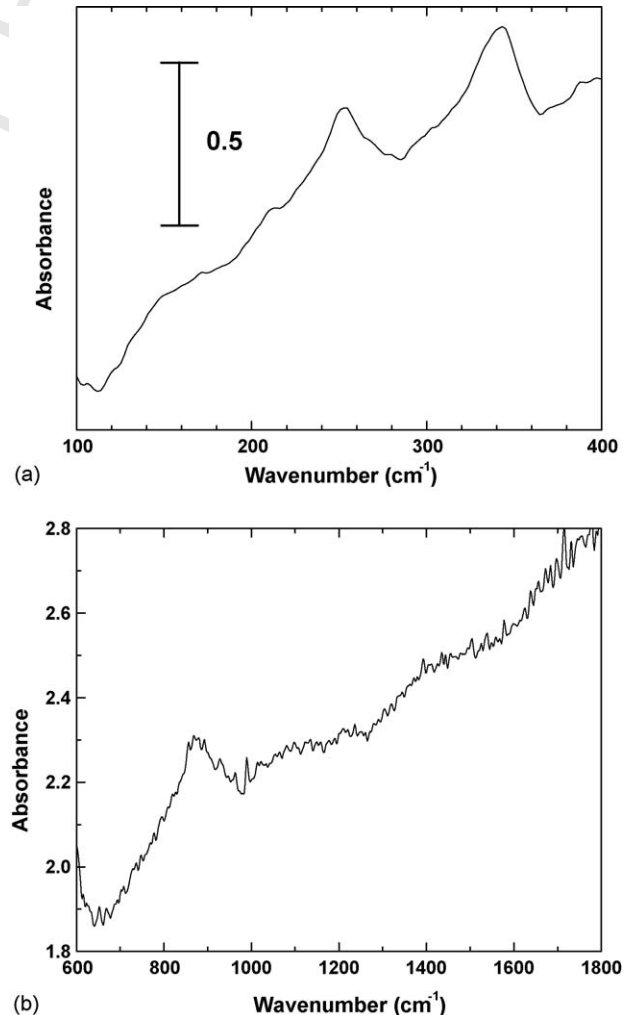


Fig. 3. Synchrotron IR spectrum of Ti_3GeC_2 (a) mid-IR and (b) far-IR region. Four of the five predicted modes are observed. The peaks observed at 210.4, 252.3 and 340.5 cm^{-1} are close to those calculated for Ti_3SiC_2 . The far-IR peak observed around 875 cm^{-1} is higher than that predicted for Ti_3SiC_2 at 607 cm^{-1} , it may be attributed to multiphonon absorptions.

4. Conclusions

In summary, the pressure dependencies of the lattice parameters of Ti_3GeC_2 , up to a pressure of 51 GPa. No phase transformations were observed. Like Ti_3SiC_2 and most other MAX phases characterized to date, the compressibility of Ti_3GeC_2 along the c axis is greater than that along the a axis. The bulk modulus is 197 ± 4 GPa, with a pressure derivative of 3.4(1). We also characterized Ti_3GeC_2 by infrared spectroscopy; four of the five expected infrared modes were observed for this material.

Acknowledgments

This work was financially supported by a grant from the National Science Foundation (DMR 0231291) and (DMR 0503711 to Drexel U.). Part of this work was conducted at Cornell High Energy Synchrotron Source (CHESS), supported by NSF grant and NIH/NIGMS under award DMR 0225180.

References

- [1] M.W. Barsoum, T. El-Raghy, *J. Am. Ceram. Soc.* 79 (1996) 1953–1956.
- [2] T. El-Raghy, A. Zavaliangos, M.W. Barsoum, S. Kalidindi, *J. Am. Ceram. Soc.* 80 (1997) 513–516.
- [3] M.W. Barsoum, T. El-Raghy, L. Ogbuji, *J. Electrochem. Soc.* 144 (1997) 2508–2516.
- [4] M.W. Barsoum, T. El-Raghy, *J. Mater. Synth. Process* 5 (1997) 197–216.
- [5] I. Salama, T. El-Raghy, M.W. Barsoum, *J. Alloys Compd.* 347 (2002) 271–278.
- [6] M.W. Barsoum, *Prog. Solid State Chem.* 28 (2000) 201–281.
- [7] M.W. Barsoum, L.H. Ho-Duc, M. Radovic, T. El-Raghy, *J. Electrochem. Soc.* 150 (2003) B166–B175.
- [8] M.W. Barsoum, T. Zhen, S. Kalidindi, M. Radovic, A. Murugaiyah, *Nat. Mater.* 2 (2003) 107–111.
- [9] E.H. Kisi, J.A.A. Crossley, S. Myhra, M.W. Barsoum, *J. Phys. Chem. Sol.* 59 (1998) 1437–1443.
- [10] M. Amer, M.W. Barsoum, T. El-Raghy, I. Wiess, S. Leclair, D. Liptak, *J. Appl. Phys.* 84 (1998) 5817–5819.

- [11] H. Wolfsgruber, H. Nowotny, F. Benesovsky, *Monatsh. Chem.* 98 (1967) 2401.
- [12] M.W. Barsoum, D. Brodtkin, T. El-Raghy, *Scrip. Met.-et. Mater.* 36 (1997) 535–541.
- [13] A. Ganguly, T. Zhen, M.W. Barsoum, *J. Alloys Compd.* 376 (2004) 287–295.
- [14] Z. Wang, C.S. Zha, M.W. Barsoum, *Appl. Phys. Lett.* 85 (2004) 3453–3455.
- [15] A. Onodera, H. Hirano, T. Yuasa, et al., *Appl. Phys. Lett.* 74 (1999) 3782–3784.
- [16] B. Manoun, S.K. Saxena, R. Gulve, et al., *Appl. Phys. Lett.* 84 (2004) 2799–2801.
- [17] H.P. Liermann, A.K. Singh, B. Manoun, S.K. Saxena, V.B. Prakapenka, G. Shen, *Int. J. Refract. Met. Hard. Mater.* 22 (2004) 129–132.
- [18] B. Manoun, S.K. Saxena, R. Gulve, et al., *Appl. Phys. Lett.* 85 (2004).
- [19] B. Manoun, S.K. Saxena, M.W. Barsoum, *Appl. Phys. Lett.* 86 (2005) 101906.
- [20] H.P. Liermann, A.K. Singh, B. Manoun, S.K. Saxena, C.S. Zha, *Int. J. Refract. Met. Hard. Mater.* 23 (2005) 109–114.
- [21] B. Manoun, R.P. Gulve, S.K. Saxena, S. Gupta, M.W. Barsoum, C.S. Zha, *Phys. Rev. B* 73 (2006) 024110.
- [22] B. Manoun, S.K. Saxena, T. El-Raghy, M.W. Barsoum, *Appl. Phys. Lett.* 88 (2006) 201902.
- [23] R.G. Greene, H. Luo, A.L. Ruoff, *Phys. Rev. Lett.* 75 (1994) 2075–2078.
- [24] A.P. Hammersley, ESRF Internal Report, ESRF97HA02T, FIT2D: An Introduction and Overview, 1997.
- [25] A.P. Hammersley, S.O. Svensson, M. Hanfland, A.N. Fitch, D. Häusermann, *High Pressure Res.* 14 (1996) 235–248.
- [26] Z. Liu, J. Hu, H. Yang, H.K. Mao, R.J. Hemley, *J. Phys.: Condens. Matter* 14 (2002) 10641.
- [27] Z. Liu, H.K. Mao, R.J. Hemley, unpublished.
- [28] F. Birch, *J. Geophys. Res.* 83 (1978) 1257.
- [29] P. Finkel, B. Seaman, K. Harrell, J. Palma, J.D. Hettinger, S.E. Lofland, A. Ganguly, M.W. Barsoum, Z. Sun, Sa. Li, R. Ahuja, *Phys. Rev. B* 69 (2004) 144108.
- [30] Y.C. Zhou, Z.M. Sun, X.H. Wang, S.Q. Chen, *J. Phys.: Condens. Matter* 13 (2001) 10001.
- [31] H.G. Drikamer, R.W. Lynch, R.L. Clendenen, E.A. Perez-Alubuerne, in: F. Seitz, D. Turnbull (Eds.), *Solid State Physics*, vol. 19, Academic, NY, 1996, p. 135.
- [32] J.Y. Wang, Y.C. Zhou, *Phys. Rev. B* 69 (2004) 144108.